DOI: 10.1002/ejoc.200800832

Solid-State Fluorescence Changes of 2-(4-Cyanophenyl)-5-[4-(diethylamino)-phenyl]-3*H*-imidazo[4,5-*a*]naphthalene upon Inclusion of Organic Solvent Molecules

Yousuke Ooyama,*[a] Shinobu Nagano,[a] Miyako Okamura,[a] and Katsuhira Yoshida*[a]

Keywords: Dyes / Clathrates / Nitrogen heterocycles / Fluorescence / Inclusion compounds

Novel imidazo[4,5-*a*]naphthalene-type fluorescent clathrate host 2-(4-cyanophenyl)-5-[4-(diethylamino)phenyl]-3*H*-imidazo[4,5-*a*]naphthalene (**2**), with two possible tautomeric forms (**A** and **B**) of the imidazole ring, was developed. The crystal of fluorophore **2** exhibits sensitive colour change and fluorescence enhancement behaviour with a blueshift in the emission maximum upon enclathration of various kinds of organic solvent molecules. The crystal structures of the guest-free and clathrate compounds of **2** were determined by X-ray analysis. On the basis of spectroscopic data and crystal structures, the effects of the enclathrated guest on the solid-state photophysical properties of the clathrate compounds are discussed.

Introduction

Solid-state fluorescence of organic fluorescent dyes has recently attracted increasing interest, because of their many uses both in the fundamental research fields of solid-state photochemistry and polymorphism and in the applied field of optoelectronic devices.[1] For the design of desirable solid-state fluorescent materials, it is very important to obtain information about the relationship between the photophysical properties and the chemical and crystal structures of fluorophores. During the last decade some studies demonstrated that the key point in designing new organic solid-state fluorescent dyes is to remove the intermolecular interactions between fluorophores causing fluorescence quenching in molecular aggregation states. For example, the introduction of bulky substituents to the original fluorophores[2] and the construction of nonplanar structures with sterically hindered substituents[3] are known to be very useful methods for solving the problem of fluorescence quenching by molecular aggregation. As another approach, Tohnai and Miyata et al. proposed the possibility of a tunable solid-state fluorescence system consisting of an organic salt with a primary amine. In the system, the fluorescence intensity can be controlled by changing the chain length of the alkyl group on the amine.[4]

In contrast, organic fluorescent hosts that exhibit sensitive colour and fluorescence changes upon formation of host–guest inclusion complexes are useful materials for elucidation of solid-state optical properties.[5,6] Recently, Imai et al. showed that a solid-state fluorescent host system was created by self-assembly of a 2_1-helical columnar organic fluorophore composed of (1*R*,2*S*)-2-amino-1,2-diphenylethanol and fluorescent 1-pyrenecarboxylic acid. The solid-state fluorescence of this host system changes depending on the guest molecules owing to their slight variations in molecular size and shape.[7] Therefore, an organic fluorescent host can be the most promising material for the construction of desirable solid-state fluorescent system.

In our previous works, we reported novel benzofurano[3,2-*b*]naphthoquinol-type,[5] imidazo[5,4-*a*]anthraquinol-type,[8] 5-hydroxy-5-substituent-benzo[*b*]naphtho[1,2-*d*]-furan-6-one-type[9] and phenanthro[9,10-*d*]imidazole-type[10] fluorescent hosts, whose crystals exhibit a dramatic fluorescence enhancement upon inclusion of various amines, organic solvents and carboxylic acids. In particular, imidazo[5,4-*a*]anthraquinol-type fluorophores, in which two tautomeric forms (**A** and **B**) are possible for the imidazole ring, can include various kinds of organic solvent molecules in the crystalline state by changing the tautomeric form of the imidazole ring. A dramatic fluorescence enhancement and a blueshift in the absorption and fluorescence wavelength maxima are observed depending on the enclathrated guest molecules. From comparison of the X-ray crystal structures of the guest-free and clathrate compounds, it was concluded that the destruction of the π–π interactions and the intermolecular hydrogen bonds binding fluorophores by the enclathrated guest molecules are the main reason for the guest-dependent fluorescence enhancement and the blueshift in the absorption and fluores-

[a] Department of Material Science, Faculty of Science Kochi University,
Akebono-cho, Kochi 780-8520, Japan
Fax: +81-88-844-8359
E-mail: yooyama@hiroshima-u.ac.jp
kyoshida@cc.kochi-u.ac.jp

cence maxima of the crystals. Consequently, it is expected that the fluorescent hosts condensed with imidazole ring can include various kinds of organic solvent molecules and exhibit desirable solid-state fluorescent properties according to the change in the crystal structures by changing the tautomeric form of the imidazole ring.

In connection with this research, we further developed the novel imidazo[4,5-*a*]naphthalene-type fluorescent clathrate host 2-(4-cyanophenyl)-5-[4-(diethylamino)phenyl]-3*H*-imidazo[4,5-*a*]naphthalene (**2**), which exhibits tautomerism (**A** and **B**) of the imidazole ring. Here, we report sensitive colour and fluorescence changes of **2** upon enclathration of organic solvent molecules in the solid state. The X-ray crystal structures of **2** and its guest-inclusion compounds were determined, on the basis of which the enclathrated guest effects on the solid-state fluorescence properties are discussed.

Results and Discussion

In the molecular design of fluorescent clathrate hosts, it is required that specific structural units such as a rigid backbone (fluorophore skeleton), bulky substituents and anchor groups are combined.[11–13] In order to create new fluorescent clathrate hosts, we employed the imidazo[4,5-*a*]-naphthalene-type fluorophore with an imidazole ring as the anchor group. Because two tautomeric forms (**A** and **B**) are possible for the imidazole ring, it is expected that the fluorescent hosts condensed with the imidazole ring can include various kinds of organic solvent molecules and exhibit desirable solid-state fluorescent properties according to the changes in the crystal structures induced by the changing tautomeric forms. Thus, we designed and synthesized the imidazo[4,5-*a*]naphthalene-type fluorescent clathrate host 2-(4-cyanophenyl)-5-[4-(diethyllamino)phenyl]-3*H*-imidazo-[4,5-*a*]naphthalene (**2**; Scheme 1).

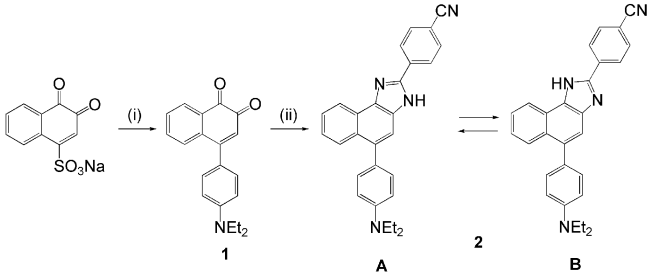

Scheme 1. (i) *N*,*N*-diethylaniline, $NiCl_2 \cdot 4H_2O$, CH_3COOH/H_2O (4:1), 7 d, room temp., 58%; (ii) *p*-cyanobenzaldehyde, CH_3COONH_4, CH_3COOH, 1 h, 80 °C, 75%.

Fluorophore **2** is conveniently synthesized as shown in Scheme 1. We first prepared 4-[4-(diethylamino)phenyl]-1,2-naphthoquinone (**1**) in 58% yield by the reaction of sodium 1,2-naphthoquinone-4-sulfonate with *N*,*N*-diethylaniline in acetic acid in the presence of nickel(II) chloride. Next, fluorophore **2** was synthesized in 58% yield by the reaction of *p*-cyanobenzaldehyde with 1,2-naphthoquinone **1** in the presence of an excess amount of ammonium acetate in acetic acid.

The absorption and fluorescence spectra of **2** in benzene are shown in Figure 1. Fluorophore **2** exhibits intense absorption bands at around 386 nm (ε_{max} = 27200 $dm^3 mol^{-1} cm^{-1}$) and a single intense fluorescence band at around 479 nm. The fluorescence quantum yield (Φ) is 0.91.

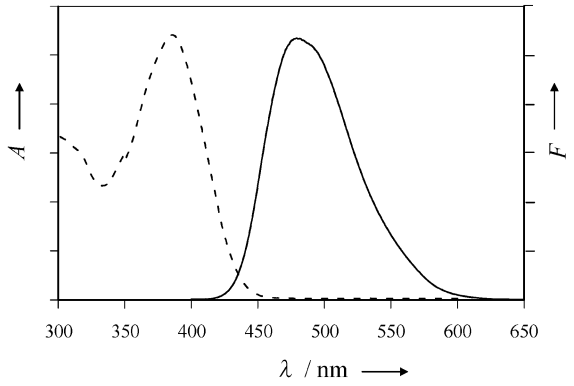

Figure 1. Normalized absorption (– – –) (2.5×10^{-5} M) and fluorescence (——) (2.5×10^{-6} M, λ_{ex} = 386 nm) spectra of **2** in benzene. Measured under oxygen-free conditions.

Inclusion Ability in the Crystalline State

In order to investigate the inclusion ability of **2**, we recrystallized fluorophore **2** from various organic solvents. We found that fluorophore **2** yields various host–guest inclusion compounds in stoichiometric ratios with organic solvent molecules such as ethanol, ethyl acetate, morpholine and 1,4-dioxane in the crystalline state. These results suggest that the imidazole ring is effective to fix guest molecules in the crystalline state. The guest-free crystal was obtained by recrystallization of **2** from acetonitrile. The characteristics of the guest-free and various inclusion crystals obtained by recrystallization of **2** are summarized in Table 1. In comparison to the guest-free crystal, the colour of the guest-inclusion crystals varied from yellowish orange to yellow and a dramatic fluorescence enhancement was observed.

Thermal analyses (TG and DTA) were performed to investigate the thermal stability of the clathrate crystals, and the thermal analysis data are shown in Table 1. The guest-release patterns were considerably different depending on the identity of the enclathrated solvent molecules, and the guest-release temperatures for the all guest-inclusion crystals were higher than their original boiling points of the guest. Interestingly, after releasing solvent molecules, only morpholine inclusion crystal showed the original melting point at around 245 °C; the morpholine inclusion crystal shows two endothermic peaks associated with the guest release and melting points. The TG and DTA profiles of the morpholine and ethanol inclusion crystals are shown in Figure 2. From the visual observation of the thermal sta-

Table 1. Host–guest molar ratio, crystal form, crystal colour and thermal analysis of the guest-free and guest-inclusion crystals of **2**.

Guest	Host/Guest (molar ratio)	Crystal form	Crystal colour	TG weight loss [%]		Guest loss endotherm peak point [°C]	Host **2** melt endotherm peak point [°C]
				Calculation	Observation		
None	1:0	Prism	Yellowish orange	0	0	–	245
Morpholine	1:1	Prism	Yellowish orange	17.29	17.23	146	245
Ethanol	1:1	Leaflet	Yellowish orange	9.96	9.63	138	–
Ethyl acetate	2:1	Needle	Yellow	9.56	9.85	159	–
1,4-Dioxane	2:1	Needle	Yellow	9.56	9.63	176	–

bility of the clathrate crystals, the morpholine inclusion crystal melted around 245 °C. In contrast, the other guest inclusion crystals melted at the temperature of guest release. It is known that some host–guest inclusion crystals melt with concomitant release of the guest; thus, it was considered that the degree of orientational disorder with the concomitant release of the guest is already close to that of the liquid.[14] Actually, comparison of the X-ray crystal structures of the guest-free and guest-inclusion compounds demonstrated that the packing structures of the guest-free and morpholine-inclusion compounds are quite similar to each other (See Figures 4 and 5). Thus, in the case of the morpholine-inclusion crystal, it was revealed that the crystal structure was not destroying after release of the guest was complete, which explained the appearance of the two endothermic peaks associated with the release of the guest and the melting points. In all the guest-released guest-inclusion crystals, the fluorescence excitation and fluorescence maxima were redshifted and their fluorescence intensities were decreased, so that the photophysical properties of the guest-released guest-inclusion crystals are close to that of the as-prepared guest-free crystal.

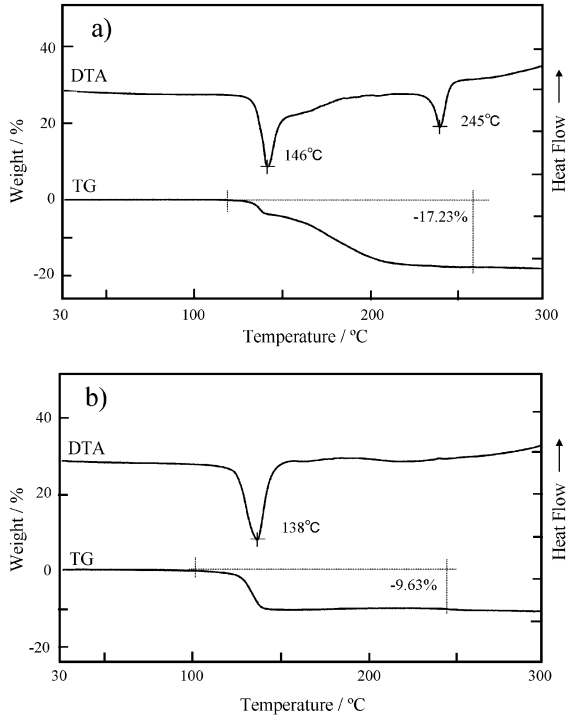

Figure 2. TG and DTA traces for the guest inclusion compounds: (a) **2**·morpholine and (b) **2**·ethanol.

Solid-State Fluorescence Enhancement Behaviour upon Formation of Guest-Inclusion Crystals

In order to investigate the effect of clathrate formation on the solid-state photophysical properties, the fluorescence excitation and emission spectra of the guest-free and guest-inclusion crystals were measured (Figure 3). In comparison to the guest-free crystal, the excitation and emission maxima of the guest-inclusion crystals exhibit a blueshift and the fluorescence intensity is enhanced to various degrees depending on the identity of the enclathrated guest molecules. However, the fluorescence intensity of the morpholine inclusion crystal is almost the same as the guest-free host crystal. The guest-free host crystal exhibits relatively weak fluorescence with an emission maximum at 536 nm, whereas the guest-inclusion crystals exhibit much stronger fluorescence intensity with the emission maximum blueshifted to around 491–517 nm. In comparison with the guest-free crystal, the fluorescence intensities of the guest-inclusion crystals were ca. 1.6-fold in ethanol-, ca. 2.1-fold in ethyl acetate- and ca. 4.8-fold in 1,4-dioxane-inclusion

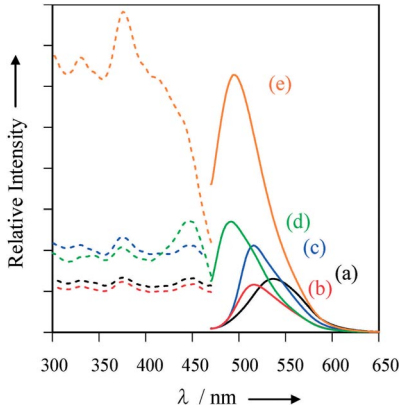

Figure 3. Solid-state excitation (– – –) and fluorescence (——) spectra of the guest-free and guest inclusion crystals of **2**: (a) **2** (guest-free): λ_{ex} = 451 nm, λ_{em} = 536 nm, Φ = 0.06; (b) **2**·morpholine: λ_{ex} = 452 nm, λ_{em} = 517 nm, Φ = 0.05; (c) **2**·ethanol: λ_{ex} = 451 nm, λ_{em} = 515 nm, Φ = 0.08; (d) **2**·ethyl acetate: λ_{ex} = 446 nm, λ_{em} = 491 nm, Φ = 0.10; (e) **2**·1,4-dioxane: λ_{ex} = 440 nm, λ_{em} = 495 nm, Φ = 0.26.

crystals. The solid-state fluorescence quantum yield (Φ) increases in the order of **2**·1,4-dioxane (Φ = 0.26) > **2**·ethyl acetate (Φ = 0.10) > **2**·ethanol (Φ = 0.08) > **2** (guest-free) (Φ = 0.06) ≈ **2**·morpholine (Φ = 0.05).

Relation between Solid-State Fluorescence Properties and X-ray Crystal Structures of Various Clathrate Compounds of 2

To understand the enclathrated guest effects on the fluorescence properties of the crystal, the crystal structures of the guest-free and guest-inclusion compounds were determined by X-ray diffraction analysis.

Figures 4–8 show the X-ray crystal structures of the guest-free and guest-inclusion compounds. The tautomeric forms (**A** and **B**) of the imidazole ring of host **2** in the crystalline state changed depending on the enclathrated guest molecules. Host **2** adopts tautomeric form **A** in the crystals of **2**·morpholine and **2**·ethanol and form **B** in the crystals of the guest-free host and **2**·1,4-dioxane. Interestingly, in the crystal of **2**·ethyl acetate, there are two crystallographically independent host molecules; one is form **A**, and the other is form **B**. These results indicate that host **2** can include various guest molecules by changing the tautomeric form of the imidazole ring. The torsion angles between the naphthoimidazole plane and the *p*-cyanophenyl group are 0.5–10° for all the compounds, which shows that the two rings are coplanar. In contrast, the *p*-diethylaminophenyl groups are twisted from the naphthoimidazole plane by about 50–70° for all the compounds.

Figures 4 and 5 show the molecular packing structure for the guest-free host and **2**·morpholine (H/G, 1:1) crystals, respectively. Both crystals are built up by the π-stacking arrangements between the naphthoimidazole rings and the *p*-cyanophenyl moieties in the two hosts. There are 16 (= 8 × 2) and 14 (= 7 × 2) short interatomic π–π contacts of less than 3.6 Å in the pair of hosts for the guest-free host and **2**·morpholine (H/G, 1:1) crystals, respectively. The average distance of the interatomic π–π contacts is ca. 3.51 Å for the guest-free compound and ca. 3.48 Å for **2**·morpholine, which suggest strong π–π interactions. In the crystal of **2**·morpholine, the intramolecular hydrogen bonds are observed between the host and the guest: the protons of the imidazole ring of **2** point towards the oxygen atom of morpholine [N(2)–H(1)···O(1) 172(2)°, N(2)···O(1) 2.881(6) Å].

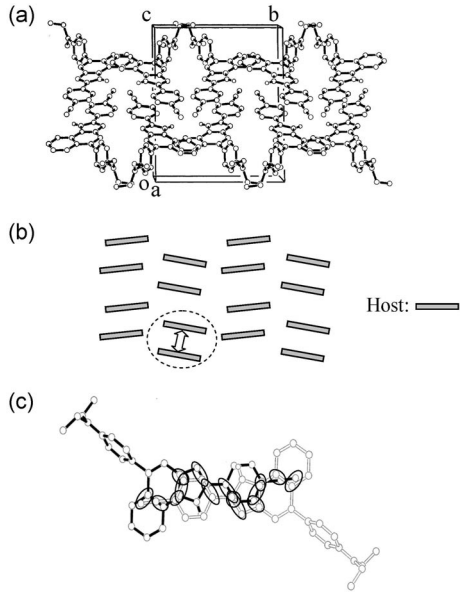

Figure 4. Crystal structure of **2**: (a) a stereoview of the molecular packing structure; (b) schematic structure; (c) top view of the pairs of fluorophores.

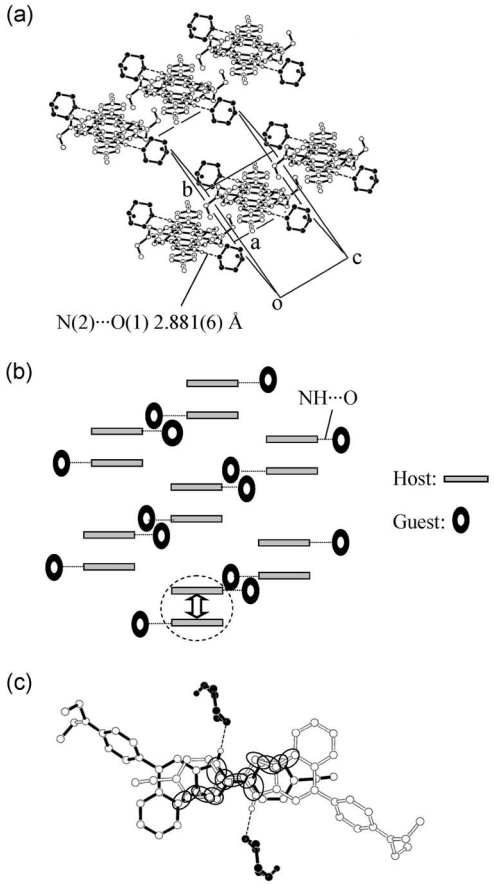

Figure 5. Crystal structure of **2**·morpholine: (a) a stereoview of the molecular packing structure; (b) schematic structure; (c) top view of the pairs of fluorophores.

In contrast, the crystal of **2**·ethanol (H/G, 1:1) is made up by the stacking arrangements that avoid short contacts between the chromophores (Figure 6). There are 4 (= 2 × 2) short interatomic contacts of less than 3.6 Å between the host molecules (Figure 6c). The average distance of the interatomic π–π contacts is ca. 3.52 Å, which is a long distance in comparison to those of the guest-free host and **2**·morpholine. A 1D chain ranging alternately host and guest (···H···G···H···) is formed through intermolecular hydrogen bonding between the hydroxy group of the ethanol molecule and the imidazole ring of the host molecule; the proton of an imidazole ring of the host is directed towards the oxygen atom of the guest [N(2)–H(1)···O(1) 159(4)°,

N(2)···O(1) 2.844(7) Å] and the hydroxy proton of the guest is directed towards an imino nitrogen atom of another host molecule [O(1)–H(25)···N(1) 172(6)°, O(1)···N(1) 2.952(6) Å], as shown in Figure 6b.

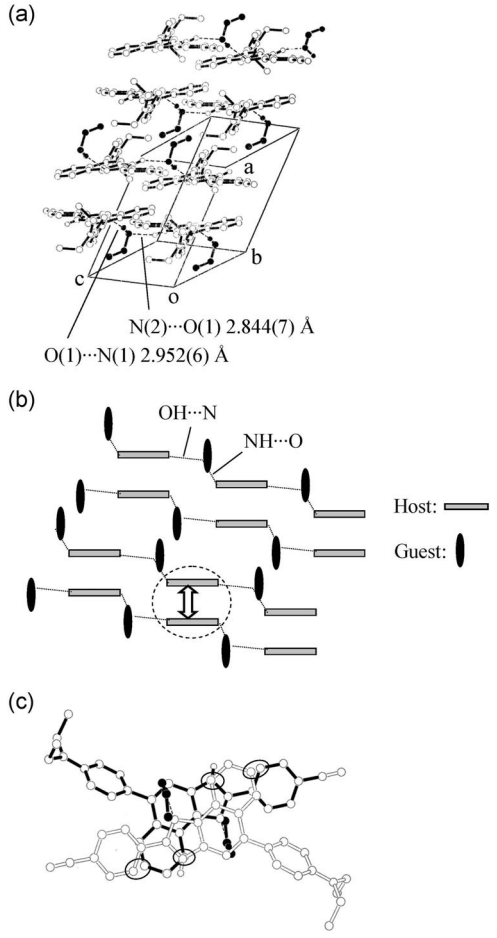

Figure 6. Crystal structure of **2**·ethanol: (a) a stereoview of the molecular packing structure; (b) schematic structure; (c) top view of the pairs of fluorophores.

Figure 7 shows the molecular packing structure for the crystal of **2**·ethyl acetate (H/G, 2:1). The crystal is made up of two types of stacking arrangements. One arrangement involves π stacking between the hosts with form **B** (Figure 7b,c: I) or form **A** (Figure 7b,d: II), and the other arrangement involves π stacking between the host with form **A** and the host with form **B** (Figure 7b,e: III): the former involves π stacking between the naphthoimidazole π planes containing the *p*-cyanophenyl moiety, and the latter involves π stacking between the imidazole rings containing the *p*-cyanophenyl moiety. There are 18, 10 and 15 short interatomic contacts of less than 3.6 Å, respectively. The average distance of the interatomic π–π contacts is ca. 3.53, 3.52 and 3.52 Å, respectively, which is a long distance in comparison with those of the guest-free host and **2**·morpholine and almost the same as that of **2**·ethanol. The enclathrated ethyl acetate molecule is bound to one host molecule through an intermolecular hydrogen bond, in which the proton of the imidazole ring of the host with form **B** is directed towards the carbonyl oxygen atom of the guest molecule [N(1)–H(1)···O(1) 177(4)°, N(1)···O(1) 2.908(5) Å]. Furthermore, the neighbouring hosts with form **A** and form **B** are connected by an intermolecular hydrogen bond between the proton of the imidazole ring and the cyano nitrogen atom [N(6)–H(25)···N(3) 161(4)°, N(6)···N(3) 3.027(7) Å].

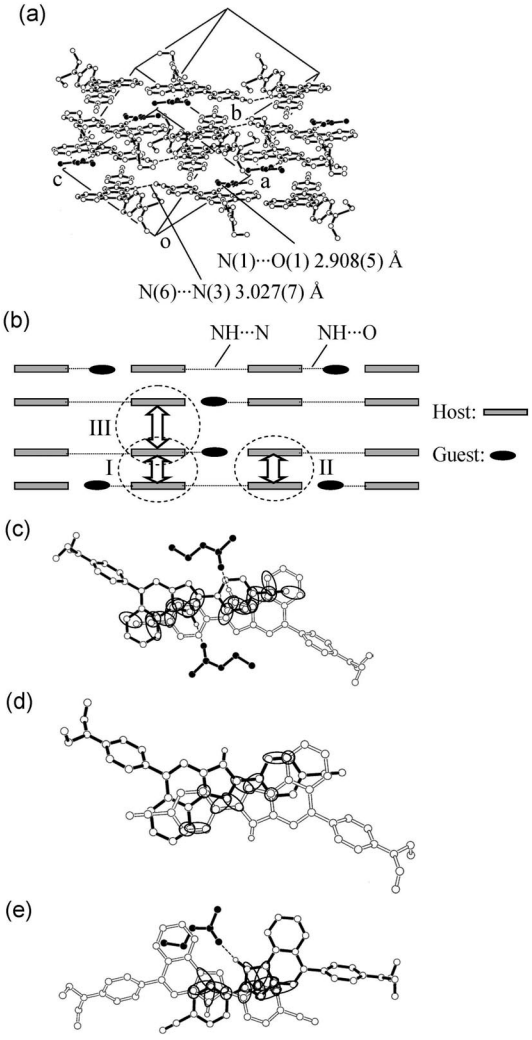

Figure 7. Crystal structure of **2**·ethyl acetate: (a) a stereoview of the molecular packing structure; (b) schematic structure; (c) top view of the pairs of fluorophores with form **B** (stacking I); (d) with form **A** (stacking II); (e) π stacking between the host with form **A** and the host with form **B** (stacking III).

Figure 8 shows the molecular packing structure for the crystal of **2**·1,4-dioxane (H/G, 2:1). The crystal is made up of two types of stacking arrangements that avoid short contacts between the chromophores. There are eight (Figure 8c: I) and four (Figure 8d: II) short interatomic contacts of less than 3.6 Å, and the average distance of the interatomic π–π contacts is ca. 3.54 and 3.57 Å, respectively, which is a large distance in comparison with those of **2**·morpholine, **2**·ethanol and **2**·ethyl acetate. The enclathrated 1,4-dioxane molecule is tightly bound to two host molecules by two intermolecular hydrogen bonds, in which the proton of the

imidazole ring of the host is directed towards the oxygen atom of the guest [N(1)–H(1)···O(1) 172(8)°, N(1)···O(1) 2.91(1) Å], which may stabilize the crystal of **2**·1,4-dioxane: the guest release temperature of **2**·1,4-dioxane is considerably higher than those of the others guest-inclusion crystals (Table 1).

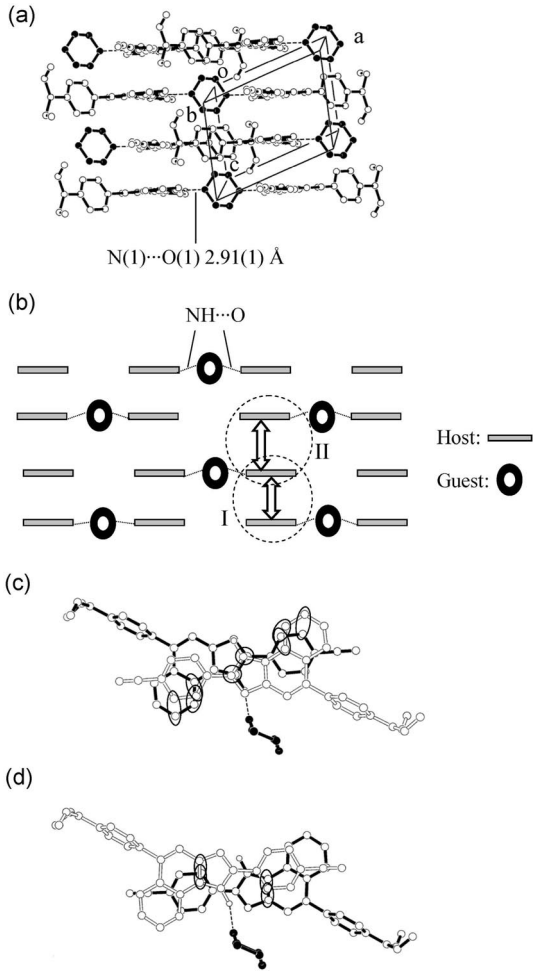

Figure 8. Crystal structure of **2**·1,4-dioxane: (a) a stereoview of the molecular packing structure; (b) schematic structure; (c) (stacking I) and (d) (stacking II) top view of the π stacking between the fluorophores.

On the basis of the solid-state photophysical data and the crystal structures of the guest-free and guest-inclusion compounds, we discuss the effects of the enclathrated guest on the solid-state photophysical properties of the clathrate compounds. A comparison of the above five crystal structures shows that the strength of the π–π interactions between the fluorophores decreases in the following order: **2** (guest-free) ≈ **2**·morpholine > **2**·ethyl acetate > **2**·ethanol > **2**·1,4-dioxane. Strong intermolecular π–π interactions between the fluorophores induce a large redshift in the absorption and fluorescence maxima and an intense fluorescence quenching in the solid state.[2,3,5,9] However, the solid-state fluorescence intensity of **2**·ethanol is weaker than that of **2**·ethyl acetate. It is considered that the continuous intermolecular hydrogen bonding ranging alternately host and guest (···H···G···H···) was only observed in **2**·ethanol, which is a principal factor leading to fluorescence quenching in the solid state. Therefore, it is confirmed from these data that the crystal of **2**·1,4-dioxane exhibits comparatively strong fluorescent intensity because of the destruction of the π–π interactions and no continuous intermolecular hydrogen bonding between hosts in comparison with the cases of **2**·morpholine, **2**·ethanol and **2**·ethyl acetate.

Conclusions

It was found that fluorophore **2** can include various guest molecules in the crystalline state by changing the tautomeric form of the imidazole ring. Solid-state fluorescence enhancement and a blueshift in the absorption and fluorescence wavelength maxima are observed depending on the enclathrated guest molecules. From comparison of the X-ray crystal structures of the guest-free and several clathrate compounds, we concluded that the differences in the destruction of the host–host π–π interactions by enclathration of the guest molecules are reflected in the solid-state fluorescence intensity and the fluorescence wavelength maxima of the crystals. Furthermore, it was found that the existence of continuous intermolecular hydrogen bonds ranging alternately fluorescent host and guest (···H···G···H···) lead to a strong solid-state fluorescence quenching behaviour. Thus, new useful information concerning the solid-state fluorescence of fluorescent organic hosts has been obtained.

Experimental Section

General: Elemental analyses were measured with a Perkin–Elmer 2400 II CHN analyzer. IR spectra were recorded with a JASCO FT/IR-5300 spectrophotometer for samples in KBr pellet form. Thermogravimetric (TG) and differential thermal analysis (DTA) spectra were performed with a Rigaku TG 8120. Single-crystal X-ray diffraction was performed with a Rigaku AFC7S diffractometer. Absorption spectra were observed with a JASCO U-best30 spectrophotometer and fluorescence spectra were measured with a JASCO FP-777 spectrophotometer. The fluorescence quantum yields (Φ) in benzene were determined by using 9,10-diphenylanthracene (Φ = 0.67, λ_{ex} = 357 nm)[15] in benzene as the standard. The solid-state fluorescence quantum yields (Φ) were determined by using a calibrated integrating sphere system (λ_{ex} = 325 nm). For the measurement of the solid-state fluorescence excitation and emission spectra of the crystals, a Jasco FP-1060 attachment was used. ^{1}H NMR spectra were recorded with a JNM-LA-400 (400 MHz) FT NMR spectrometer with tetramethylsilane (TMS) as an internal standard.

4-[4-(Diethylamino)phenyl]-[1,2]naphthoquinone (1): A solution of sodium 1,2-naphthoquinone-4-sulfonate (10.0 g, 38.4 mmol), *N*,*N*-diethylaniline (8.6 g, 57.6 mmol) and $NiCl_2$·$4H_2O$ (9.56 g, 38.4 mmol) in CH_3COOH/H_2O (4:1, 200 mL) was stirred at room temperature for 7 d. The reaction mixture was poured into water. The solution was neutralized with aqueous Na_2CO_3 and extracted with CH_2Cl_2. The organic extract was washed with water, and the solvent was evaporated. The residue was chromatographed on silica gel (CH_2Cl_2) to give **1** (6.78 g, 58%). M.p. 116–118 °C. ^{1}H NMR (400 MHz, [D$_6$]DMSO, TMS): δ = 1.13 (t, 6 H), 3.42 (m, 4 H),

6.29 (s, 1 H), 6.79 (d, J = 8.7 Hz, 2 H), 6.39 (d, J = 8.7 Hz, 2 H), 7.61 (m, 1 H), 7.72 (m, 1 H), 7.72 (m, 2 H), 8.03 (m, 1 H) ppm. IR (KBr): $\tilde{\nu}$ = 1650, 1603 cm^{-1}. MS: m/z (%) = 305 (100) $[M]^+$.

2-(4-Cyanophenyl)-5-[4-(diethylamino)phenyl]-3*H*-imidazo[4,5-*a*]-naphthalene (2): A solution of **1** (5.63 g, 18.45 mmol), *p*-cyanobenzaldehyde (2.42 g, 18.5 mmol) and ammonium acetate (22.75 g, 0.3 mol) in acetic acid (170 mL) was stirred at 80 °C for 1 h. The reaction mixture was neutralized with aqueous Na_2CO_3 and extracted with CH_2Cl_2. The organic extract was washed with water, and the solvent was evaporated. The residue was chromatographed on silica gel (CH_2Cl_2/ethyl acetate, 10: 1) to give **2** (5.75 g, 75%). M.p. 244–247 °C. ^{1}H NMR (400 MHz, [D$_6$]DMSO, TMS): δ = 1.15 (t, 6 H), 3.34 (m, 4 H), 6.80 (d, J = 8.5 Hz, 2 H), 7.31 (d, J = 8.3 Hz, 2 H), 7.46 (m, 1 H), 7.54 (s, 1 H), 7.65 (m, 1 H), 7.96 (d, J = 8.3 Hz, 1 H), 8.04 (d, J = 8.1 Hz, 2 H), 8.41 (d, J = 7.8 Hz, 2 H), 8.58 (d, J = 6.6 Hz, 1 H) ppm. IR (KBr): $\tilde{\nu}$ = 2220 cm^{-1}. $C_{28}H_{34}N_4$ (426.60): calcd. C 80.74, H 5.81, N 13.45; found C 80.88, H 5.61, N 13.68.

Preparation of Guest-Inclusion Crystals: Host compound **2** was dissolved with heating in the respective guest solvent. The solution was filtered and kept for a few days at room temperature. The crystals that formed were collected by filtration. The host (H)/guest (G) stoichiometric ratio of the inclusion compounds was determined by ^{1}H NMR integration and C, H, N analysis.

2 (Guest-Free): Host **2** (500 mg) was dissolved by warming in nitromethane (26 mL), and the resulting solution was allowed to stand at room temperature. The crystals (orange-yellow, prism, 340 mg) were collected and dried on the filter paper.

2·Morpholine (H/G, 1:1): Host **2** (200 mg) was dissolved by warming in morpholine (3 mL), and the resulting solution was allowed to stand at room temperature. The crystals (yellow, prism, 184 mg) were collected and dried on the filter paper. $C_{32}H_{33}N_5O$ (503.65): calcd. C 76.31, H 6.60, N 13.91; found C 76.02, H 6.97, N 14.23.

2·Ethyl Acetate (H/G, 2:1): Host **2** (100 mg) was dissolved by warming in ethyl acetate (2 mL), and the resulting solution was allowed to stand at room temperature. The crystals (yellow, needle, 70 mg) were collected and dried on the filter paper. $C_{60}H_{56}N_8O_2$ (921.15): calcd. C 78.23, H 6.13, N 12.16; found C 78.43, H 6.17, N 12.32.

2·Ethanol (H/G, 1:1): Host **2** (420 mg) was dissolved by warming in ethanol (18 mL), and the resulting solution was allowed to stand at room temperature. The crystals (yellow, leaflet, 322 mg) were collected and dried on the filter paper. $C_{30}H_{30}N_4O$ (462.59): calcd. C 77.89, H 6.54, N 12.11; found C 77.60, H 6.24, N 11.92.

2·1,4-Dioxane (H/G, 2:1): Host **2** (300 mg) was dissolved by warming in 1,4-dioxane (4 mL), and the resulting solution was allowed to stand at room temperature. The crystals (yellow, needle-like, 188 mg) were collected and dried on the filter paper. $C_{60}H_{56}N_8O_2$ (921.15): calcd. C 78.23, H 6.13, N 12.16; found C 78.39, H 6.05, N 12.26.

X-ray Crystallographic Studies: The reflection data were collected at 23 ± 1 °C with a Rigaku AFC7S four-circle diffractometer by 2θ–ω scan technique and by using graphite-monochromated Mo-K_α (λ = 0.71069 Å) radiation at 50 kV and 30 mA. In all cases, the data were corrected for Lorentz and polarization effects. A correction for secondary extinction was applied. The reflection intensities were monitored by three standard reflections for every 150 reflections. An empirical absorption correction based on azimuthal scans of several reflections was applied. All calculations were performed by using the teXsan[16] crystallographic software package of Molecular Structure Corporation. CCDC-692724 (for **2**), -692725 (for **2**·morpholine), -692726 (for **2**·ethyl acetate), -692727 (for **2**·ethanol) and -692728 (for **2**·1,4-dioxane) contain the supplementary crystallographic data for this paper. These data can be obtained free of charge from The Cambridge Crystallographic Data Centre via www.ccdc.cam.ac.uk/data_request/cif.

Crystal of 2: The transmission factors ranged from 0.98 to 1.00. The crystal structure was solved by direct methods by using SIR 92.[17] The structures were expanded by using Fourier techniques.[18] Non-hydrogen atoms were refined anisotropically. Some hydrogen atoms were refined isotropically, the rest were fixed geometrically and not refined. Crystallographic data: $C_{28}H_{34}N_4$, M = 416.52, monoclinic, a = 11.665(2) Å, b = 12.531(2) Å, c = 15.743(2) Å, β = 107.38(1)°, U = 2196.2(6) Å^3, $\rho_{calcd.}$ = 1.260 g cm^{-3}, T = 296.2 K, space group $P2_1/a$ (no.14), Z = 4, μ(Mo-K_α) = 0.76 cm^{-1}, 4078 reflections measured, 3868 unique (R_{int} = 0.023), which were used in all calculations. The final R indices [$I > 2\sigma(I)$], R_1 = 0.053, $wR(F^2)$ = 0.1185.

Crystal of 2·Morpholine: The transmission factors ranged from 0.00 to 1.00. The crystal structure was solved by direct methods by using SIR 92.[17] The structures were expanded by using Fourier techniques.[18] Non-hydrogen atoms were refined anisotropically. Some hydrogen atoms were refined isotropically, the rest were fixed geometrically and not refined. Crystallographic data: $C_{32}H_{33}N_5O$, M = 503.65, triclinic, a = 10.786(3) Å, b = 16.031(7) Å, c = 8.461(2) Å, α = 98.18(3)°, β = 90.26(2)°, γ = 74.17(2)°, U = 1392.3(8) Å^3, $\rho_{calcd.}$ = 1.201 g cm^{-3}, T = 296.2 K, space group $P\bar{1}$ (no.2), Z = 2, μ(Mo-K_α) = 0.75 cm^{-1}, 5081 reflections measured, 5078 unique (R_{int} = 0.026), which were used in all calculations. The final R indices [$I > 2\sigma(I)$], R_1 = 0.0638, $wR(F^2)$ = 0.1406.

Crystal of 2·Ethyl Acetate: The transmission factors ranged from 0.95 to 1.00. The crystal structure was solved by direct methods by using SAPI 90.[19] The structures were expanded by using Fourier techniques.[18] Non-hydrogen atoms were refined anisotropically. Some hydrogen atoms were refined isotropically, the rest were fixed geometrically and not refined. Crystallographic data: $C_{60}H_{56}N_8O_2$, M = 921.15, triclinic, a = 13.153(2) Å, b = 18.937(2) Å, c = 11.983(2) Å, α = 100.55(1)°, β = 114.918(10)°, γ = 101.35(1)°, U = 2532.5(7) Å^3, $\rho_{calcd.}$ = 1.208 g cm^{-3}, T = 296.2 K, space group $P\bar{1}$ (no.2), Z = 2, μ(Mo-K_α) = 0.75 cm^{-1}, 9340 reflections measured, 9336 unique (R_{int} = 0.018), which were used in all calculations. The final R indices [$I > 2\sigma(I)$], R_1 = 0.0727, $wR(F^2)$ = 0.1699.

Crystal of 2·Ethanol: The transmission factors ranged from 0.93 to 1.00. The crystal structure was solved by direct methods by using SAPI 91.[20] The structures were expanded by using Fourier techniques.[18] Non-hydrogen atoms were refined anisotropically. Some hydrogen atoms were refined isotropically, the rest were fixed geometrically and not refined. Crystallographic data: $C_{30}H_{30}N_4O$, M = 462.59, triclinic, a = 10.364(3) Å, b = 17.680(4) Å, c = 7.444(3) Å, α = 98.23(3)°, β = 107.68(3)°, γ = 98.72(2)°, U = 1258.2(8) Å^3, $\rho_{calcd.}$ = 1.221 g cm^{-3}, T = 296.2 K, space group $P\bar{1}$ (no.2), Z = 2, μ(Mo-K_α) = 0.75 cm^{-1}, 4801 reflections measured, 4431 unique (R_{int} = 0.049), which were used in all calculations. The final R indices [$I > 2\sigma(I)$], R_1 = 0.0716, $wR(F^2)$ = 0.1760.

Crystal of 2·1,4-Dioxane: The transmission factors ranged from 0.88 to 1.00. The crystal structure was solved by direct methods by using SIR 92.[17] The structures were expanded by using Fourier techniques.[18] Non-hydrogen atoms were refined anisotropically. Some hydrogen atoms were refined isotropically, the rest were fixed geometrically and not refined. Crystallographic data: $C_{30}H_{28}N_4O$, M = 460.58, triclinic, a = 9.36(1) Å, b = 19.14(1) Å, c = 7.355(3) Å, α = 91.70(5)°, β = 107.67(6)°, γ = 86.17(8)°, U = 1253(1) Å^3, $\rho_{calcd.}$

= 1.221 g cm^{-3}, T = 296.2 K, space group $P\bar{1}$ (no.2), Z = 2, μ(Mo-K_α) = 0.75 cm^{-1}, 4705 reflections measured, 4699 unique (R_{int} = 0.110), which were used in all calculations. The final R indices [$I > 2\sigma(I)$], R_1 = 0.1533, $wR(F^2)$ = 0.3070.

Acknowledgments

This work was partially supported by a Grant-in-Aid for Science and Research from the Ministry of Education, Science Sport and Culture of Japan (Grant 18350100) and by a Special Research Grant for Green Science from Kochi University.

[1] a) C. W. Tang, S. A. Vanslyke, *Appl. Phys. Lett.* **1987**, *51*, 913–915; b) L. S. Sapochak, F. E. Benincasa, R. S. Schofield, J. L. Baker, K. K. C. Riccio, D. Fogarty, H. Kohlmann, K. F. Ferris, P. E. Burrows, *J. Am. Chem. Soc.* **2002**, *124*, 6119–6125; c) C. J. Tonzola, M. M. Alam, W. K. Kaminsky, S. A. Jenekhe, *J. Am. Chem. Soc.* **2003**, *125*, 13548–13558; d) Y. Sonoda, Y. Kawanishi, T. Ikeda, M. Goto, S. Hayashi, N. Tanigaki, K. Yase, *J. Phys. Chem. B* **2003**, *107*, 3376–3383; e) Y. Kim, J. Bouffard, S. E. Kooi, T. M. Swager, *J. Am. Chem. Soc.* **2005**, *127*, 13726–13731; f) H. Zhang, Z. Zhang, K. Ye, J. Zhang, Y. Wang, *Adv. Mater.* **2006**, *18*, 2369–2372; g) E. Sakuda, K. Tsuge, Y. Sasaki, N. Kitamura, *J. Phys. Chem. B* **2005**, *109*, 22326–22331; h) C.-H. Zhao, A. Wakamiya, Y. Inukai, S. Yamaguchi, *J. Am. Chem. Soc.* **2006**, *128*, 15934–15935; i) Z. Ning, Z. Chen, Q. Zhang, Y. Yan, S. Qian, Y. Cao, H. Tian, *Adv. Funct. Mater.* **2007**, *17*, 3799–3807; j) R. Davis, N. S. S. Kumar, S. Abraham, C. H. Suresh, N. P. Rath, N. Tamaoki, S. Das, *J. Phys. Chem. C* **2008**, *112*, 2137–2146; k) N. S. S. Kumar, S. Varghese, N. P. Rath, S. Das, *J. Phys. Chem. C* **2008**, *112*, 8429–8437.

[2] a) H. Langhals, T. Potrawa, H. Nöth, G. Linti, *Angew. Chem. Int. Ed. Engl.* **1989**, *28*, 478–480; b) H. Langhals, R. Ismael, O. Yürük, *Tetrahedron* **2000**, *56*, 5435–5441; c) K. Yoshida, Y. Ooyama, H. Miyazaki, S. Watanabe, *J. Chem. Soc. Perkin Trans. 2* **2002**, 700–707; d) Y. Ooyama, T. Nakamura, K. Yoshida, *New J. Chem.* **2005**, *29*, 447–456; e) Y. Ooyama, T. Okamoto, T. Yamaguchi, T. Suzuki, A. Hayashi, K. Yoshida, *Chem. Eur. J.* **2006**, *12*, 7827–7838; f) Y. Ooyama, Y. Harima, *Chem. Lett.* **2006**, 902–903; g) Y. Ooyama, Y. Kagawa, Y. Harima, *Eur. J. Org. Chem.* **2007**, *22*, 3613–3621; h) Y. Ooyama, T. Mamura, K. Yoshida, *Eur. J. Org. Chem.* **2007**, *30*, 5010–5019; i) Y. Ooyama, T. Mamura, K. Yoshida, *Tetrahedron Lett.* **2007**, *48*, 5791–5793.

[3] a) H.-C. Yeh, W.-C. Wu, Y.-S. Wen, D.-C. Dai, J.-K. Wang, C.-T. Chen, *J. Org. Chem.* **2004**, *69*, 6455–6462; b) Y. Ooyama, S. Yoshikawa, S. Watanabe, K. Yoshida, *Org. Biomol. Chem.* **2006**, *4*, 3406–3409; c) Y. Ooyama, S. Yoshikawa, S. Watanabe, K. Yoshida, *Org. Biomol. Chem.* **2007**, *5*, 1260–1269.

[4] Y. Mizobe, N. Tohnai, M. Miyata, Y. Hasegawa, *Chem. Commun.* **2005**, 1839–1841.

[5] a) K. Yoshida, H. Miyazaki, Y. Miura, Y. Ooyama, S. Watanabe, *Chem. Lett.* **1999**, 837–838; b) K. Yoshida, Y. Ooyama, S. Tanikawa, S. Watanabe, *Chem. Lett.* **2000**, 714–715; c) K. Yoshida, Y. Ooyama, S. Tanikawa, S. Watanabe, *J. Chem. Soc. Perkin Trans. 2* **2002**, 708–714.

[6] a) Z. Fei, N. Kocher, C. J. Mohrschladt, H. Ihmels, D. Stalke, *Angew. Chem. Int. Ed.* **2003**, *42*, 783–787; b) J. L. Scott, T. Yamada, K. Tanaka, *New J. Chem.* **2004**, *28*, 447–450.

[7] Y. Imai, K. Murata, K. Kawaguchi, T. Sato, N. Tajima, R. Kuroda, Y. Matsubara, *Chem. Asian J.* **2008**, *3*, 625–629.

[8] a) K. Yoshida, J. Yamazaki, Y. Tagashira, S. Watanabe, *Chem. Lett.* **1996**, 9–10; b) K. Yoshida, T. Tachikawa, J. Yamasaki, S. Watanabe, S. Tokita, *Chem. Lett.* **1996**, 1027–1028; c) Y. Ooyama, K. Yoshida, *New J. Chem.* **2005**, *29*, 1204–1212.

[9] Y. Ooyama, K. Yoshida, *Eur. J. Org. Chem.* **2008**, *15*, 2564–2570.

[10] K. Yoshida, K. Uwada, H. Kumaoka, L. Bu, S. Watanabe, *Chem. Lett.* **2001**, 808–809.

[11] a) E. Weber, M. Czugler in *Topics in Current Chemistry: Vol. 149: Molecular and Molecular Recognition-Clathrates I and II* (Ed.: E. Weber), Springer, Berlin, **1988**, p. 45; b) E. Weber in *Inclusion Phenomena and Molecular Recognition* (Ed.: J. L. Atwood), Plenum, New York, **1990**, vol. 4, p. 188.

[12] F. Toda, *Acc. Chem. Res.* **1995**, *28*, 480–486.

[13] K. Ochiai, Y. Mazaki, S.-I. Nishikiori, K. Kobayashi, S. Hayashi, *J. Chem. Soc. Perkin Trans. 2* **1996**, 1139–1145.

[14] a) S. A. Bourne, L. Hohnson, C. Marais, L. R. Nassimbeni, E. Weber, K. Skobridis, F. Toda, *J. Chem. Soc. Perkin Trans. 2* **1991**, 1707–1713; b) I. Csöregh, E. Weber, L. R. Nassimbeni, O. Gallardo, N. Dörpinghaus, A. Ertan, A. A. Bourne, *J. Chem. Soc. Perkin Trans. 2* **1993**, 1775–1782; c) J. D. Wright, *Molecular Crystals*, 2nd ed. Cambridge University Press, New York, **1995**, p. 32.

[15] C. A. Heller, R. A. Henry, B. A. Mclaughlin, D. E. Bills, *J. Chem. Eng. Data* **1974**, *19*, 214–219.

[16] *teXsan: Crystal Structure Analysis Package*, Molecular Structure Corporation, **1985** and **1992**.

[17] A. Altomare, M. C. Burla, M. Camalli, M. Cascarano, C. Giacovazzo, A. Guagliardi, G. Polidori, *J. Appl. Crystallogr.* **1994**, *27*, 435.

[18] P. T. Beurskens, G. Admiraal, G. Beurskens, W. P. Bosman, R. de Gelder, R. Israel, J. M. M. Smits, *The DIRIF94 Program System*, Technical Report of the Crystallography Laboratory, University of Nijmegen, The Netherlands, **1994**.

[19] Fan Hai-Fu, *Structure Analysis Programs with Intelligent Control*, Rigaku Corporation, Tokyo, Japan, **1990**.

[20] Fan Hai-Fu, *Structure Analysis Programs with Intelligent Control*, Rigaku Corporation, Tokyo, Japan, **1991**.

Received: August 29, 2008
Published Online: November 5, 2008

